Verification techniques for the assessment of SBAS integrity performances: a detailed analysis using both ESTB and WAAS broadcast signals

Michel Maria Mathias Tossaint, Juan Carlos De Mateo, Pedro Dias Freire Da Silva, Javier Ventura-Traveset
European Space Agency, ESTEC, The Netherlands

1 BIOGRAPHY

M.M.M. Tossaint graduated as a M.Sc. in Aerospace Engineering from Delft Univ. of Technology (The Netherlands) in 1997. He joined the Space Systems Department of the Dutch NLR in 1998, where he was involved in both EGNOS and Galileo Safety, Verification and Validation issues. Currently, he is working for ESA in the Navigation and TT&C Section of the department of Telecommunications. There he is involved in the European Geostationary Navigation Overlay System (EGNOS) safety related research and application development.

J.C. De Mateo is a graduate in Telecommunications from the Polytechnics Univ. at Madrid (Spain). He has worked in the design of radio-frequency circuits before joining ESA to support EGNOS and Galileo developments as a navigation engineer.

P.D.F. Da Silva is a graduate in Aerospace Engineering in avionics from Instituto Superior Técnico at Lisbon (Portugal) in 2000. He is currently working in the Navigation and TT&C Section as a Young Graduate Trainee involved in EGNOS applications.

Dr J. Ventura-Traveset holds a MS in Telecom. Engineering from the Polytechnic Univ. of Catalonia (Barcelona, Spain, 1988); a M.S.E in Signal Processing by Princeton Univ. (Princeton, NJ, USA) in 1992; and a PhD in Electrical Engineering by the Polytechnic of Turin (Italy) in 1996. Since March 1989, he is working at the European Space Agency (ESA), involved in mobile, fix, earth observation and satellite navigation programs. He is currently Principal System Engineer of the EGNOS project.

2 ABSTRACT

In this article, system verification techniques that allow assessing SBAS integrity performances are described and tested. These techniques, proposed to be used also on the final EGNOS system, are evaluated here, using both the EGNOS System Test Bed (ESTB) and the Wide Area Augmentation System (WAAS) broadcast signals. As a spin-off of this analysis we also assess some differences between ESTB and WAAS systems. It is shown that, despite the limited number of reference stations, the ESTB reaches meter accuracies and provides good protection levels. These encouraging results pave the way to a sound introduction of EGNOS System operations in 2004.

3 INTRODUCTION

The section of radio navigation and TT&C within the ESA Directorate of Technical and Operational Support (DTOS), supports the ESA GNSS-1 EGNOS Project Office in Toulouse on different system engineering activities, including the assessment of verification techniques. This research work is complementary to the continuous ESTB performance assessment done by other important Research Centres such as CNES (France), NMA (Norway), EUROCONTROL and industry.

The ESTB, a pre-operational EGNOS signal, is available since early 2000 for navigation demonstrations and service trials [ESTB]. The main objectives of the ESTB are: to have an assessment of the global performance that EGNOS can achieve; to analyse with detail critical design issues or tradeoffs between several options; to demonstrate the system operation to the final users; and to develop and validate system test methods. In this study, we make use of the ESTB signal to assess the effectiveness of some verification techniques, which are proposed to be applied to EGNOS SIS, during the system validation and qualification. Within the EGNOS project Thales ATM is responsible for the Assembly Integritation & Verification.

The Horizontal and Vertical Protection Levels (XPL), which are computed from broadcast EGNOS messages, to protect users from potential degradation of the GPS system, expressed in terms of Horizontal and Vertical Navigation Error (XNSE) above a certain user level, called the Alert Limit (XAL). Several cases for the relation between XNSE, XAL and XPL exist, however, two cases are very important from a safety perspective:

1. XPL<XNSE<XAL: System is available but not safe, not leading to a hazardous situation, called Misleading Information (MI)

2. XPL<XAL<XNSE: System is available but not safe and leading to a hazardous situation, called Hazardous Misleading Information (HMI)

Both cases are considered as an SBAS out of tolerance condition, and are assumed in EGNOS as non-integrity events. The EGNOS system will guarantee that the probability of occurrence of those events is below $2x10^{-7}$ in 150 seconds.

Potential error sources that may provoke these out of tolerance conditions include:

- Fast and Slow correction / User Differential Range Error (UDRE) mismodelling
- Grid Ionospheric Vertical Delay (GIVD) / Grid Ionospheric Vertical Error (GIVE) mismodelling
- Extensive local errors (multipath and/or receiver noise (due to interference))

It is assumed here that the contribution to XPL out-of tolerance of tropospheric underbounding errors at the receiver is negligible.

This paper describes a specific verification methodology to assess the individual bounding capabilities of UDRE/GIVE/Local error bounds. The practical implementation of this methodology and its effectiveness is demonstrated using both ESTB and WAAS broadcast signals.

4 DESCRIPTION OF METHODOLOGY

For each of the error sources described in the introduction, periods of MI will be analysed. Each of these investigations requires some reference source of the real values. The first two techniques described in the next sections depend on data, gathered by the International Geodetic Survey (IGS), and processed by the Centre for Orbit Determination (CODE) Institute in Bern (Switzerland). As such, this reference has a disadvantage that it might not be totally independent, but on the other hand the advantage is that the data is highly accurate, available through Internet, and has coverage over the entire globe. The truth data of any verification has to be in the same order, or better, of magnitude in accuracy. Therefore the analysis starts with an estimation of the accuracy of the reference data.

4.1 SATELLITE ORBIT AND CLOCK INFORMATION

Since the SBAS orbit and clock correction accuracy depends on location within the service area, a so-called Satellite Residual at Worst User (SREW) location σ_{SREW} is defined as the real error associated with this data. The accuracy required for the reference source is estimated as follows. With a minimum UDRE value of 1m, set as a practical limit on the minimum value to be broadcast, the truth value for σ_{SREW} should have an accuracy of about 1/ $3.29\sigma = 0.3$m (1σ).

This requirement is actually feasible with IGS data. Post-processing data from a number of ground stations, higher than the number of EGNOS ground stations, will in principle, lead to a better orbit and clock solution. Currently, the accuracy of the CODE solution is about 5cm (1σ) [IGS01] for combined satellite position and time.

The principle idea to compute the SREW is to find the real range correction to the GPS solution. This can be constructed from the IGS clock and orbit information, by converting this to the pseudorange domain. At the same time the EGNOS corrections have to be converted to a single range correction, after which the two can be compared to find the SREW. Two main obstacles have to be over come before doing so.

First, the time frame offset between EGNOS and IGS has to be found. The clock solutions of IGS are relative to a 'derived' time frame called the IGS Network Time (INT), the same is valid for the EGNOS corrections (ENT). Note that the IGS time frame is synchronised to the GPS time frame on a daily basis, and is stable to within a few nanoseconds. To find the offset between INT (or GPS) and ENT, not only the clock, but also the clock and ephemeris corrections have to be synchronised, because this information can not be determined separately in SBAS.

The accuracy of the method is assessed as follows. The mean number of satellites being monitored by the CPF is assumed to be equal to 9 and the UDRE budget to be 1.3m (2σ). Assuming also that the combined constellation orbit & clock correction values have a zero mean and that single satellite orbit & clock corrections have equal variance, the combined variance is, according to the Gaussian propagation law for independent samples, equal to 1.3/sqrt(9)=0.43m. Filtering 100 independent

measurements over time finally, leads to an estimation of the accuracy of ENT-INT of 0.04m. Together with the accuracy of the CODE data mentioned earlier, it must be evident that the requirement of 0.3m can be met.

The fact that there is only one UDRE value for a satellite all over the European Civil Aviation Conference (ECAC) area, has some limitations because an orthogonal correction has to be translated to a range correction depending on the location within ECAC (slow corrections). The UDRE represents the remaining error at the Worst User Location (WUL), but is valid for the entire ground visibility area of the satellite. The theoretical variation of the SREW over the ECAC area (80 by 50 deg) is illustrated in Figure 4-1. This figure shows the delta range correction as a function of the position within ECAC for a satellite at (0,0,20e6) and a slow correction of (1/√3, 1/√3, 1/√3). The figure shows that the range correction can vary about 0.5m for a slow correction with a norm of 1m.

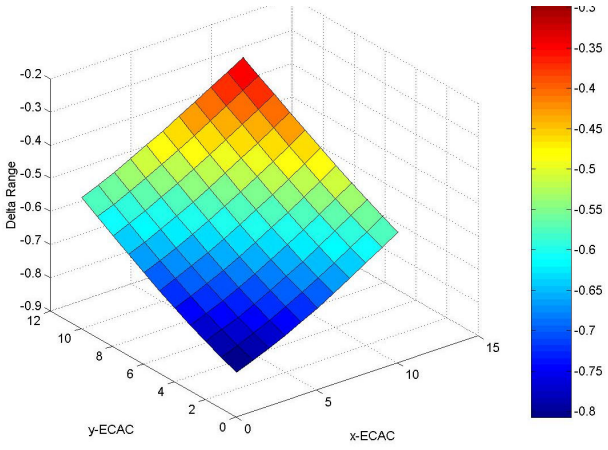

Figure 4-1 Maximum sensitivity case of user location to slow correction transfer into range correction

The solution to the problem of finding the WUL, however, is easy to implement in an algorithm. The SREW-UDRE error can be computed for a certain grid over the visibility area of the satellite and the maximum is simply selected.

4.2 IONOSPHERIC INFORMATION

The minimal requirement on the accuracy of the 'real User Ionospheric Vertical Error' $\sigma_{UIVE,truth}$ is established in a similar way as the σ_{SREW}. With the minimum UIVE value of 0.9m, set as a practical limit on the minimum value to be broadcast, the truth value should have an accuracy of about 0.9/ 3.29 = 0.27m (1σ). This requirement will be met with using the CODE data, as will be shown later.

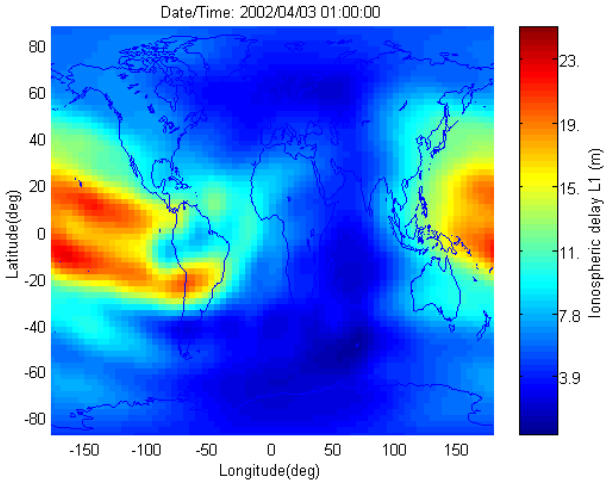

Figure 4-2 Example of CODE Ionosphere data

Data from several stations can be combined to fit a model to the slant TEC measurements in a least squares or Kalman filter (for real-time applications). Simultaneously, the receiver and satellite biases can be determined (with at least one or more known receiver biases). CODE provides such data which is available almost in real time, with a period of 2 hours. As an example see Figure 4-2 which shows the Total Electronic Content (TEC) of the ionosphere over the globe. The grid spacing is 2.5° in latitude and 5° in longitude. The maps are provided in the IONospheric EXchange format (IONEX) [ION01.

The accuracy of the values at the grid points is estimated to have a maximum (99%) of about 5 TEC units or 0.9m [IGS99] derived from the deviance of the single solution of an Analysis Centre to the combined solution. With the Gaussian assumption, the $\sigma_{UIVE,truth}$ reference value is estimated at 0.9/3=0.3m (1σ). Unfortunately, these maps have a limited resolution, both in time and space, an interpolation routine has to be used, which means that ionospheric irregularities (with high spatial and temporal gradients) could remain undiscovered.

The method of verification is now relatively simple. The SBAS ionospheric data can be computed once full map data is available. IGS information is interpolated over time to the epochs of receiving a SBAS message with ionospheric delays. At the same time this information is interpolated in space to the grid points of the SBAS.

Another verification technique to be mentioned is to use the measurements itself, the dual frequency solution. However, since this method is limited to the Ionospheric Pierce Points (IPP) and does not give information about all the supported Ionospheric Grid Points (IGP), this method is not used here. Although, it is also proposed to be used during EGNOS validation to assess the EGNOS ionospheric slant delays bounding.

4.3 MULTIPATH AND RECEIVER NOISE

Code multipath and noise can be calculated from real code and phase measurements on L1 and L2. The combined of code multipath and receiver noise is found from the code minus phase observable, and making the assumption that phase multipath and noise are much smaller than code multipath and noise. This observable also contains the ionospheric delay and the ambiguity on the phase. The exact value of the ionospheric delay is found from the dual frequency measurement on L1 and L2, after correction of the cycle slips and applying the satellite and receiver inter-frequency biases. The observable can be shifted with a constant so that the observable is zero mean over a satellite pass in order to correct for the unknown ambiguities. This also requires cycle slip free measurements, which are relatively easy to obtain with static data in post-processing.

5 APPLICATION OF METHODOLOGY TO ESTB SIGNAL IN SPACE

This section will make use of the ESTB signal to demonstrate that the methodology described in the previous section works, when applied to real SBAS broadcast data.

Data was recorded at ESA Space Research Centre, ESTEC in Noordwijk, The Netherlands, on 03-04-2002. During a period of about 12 hours the data showed no MI. This is illustrated in Figure 5-1, where there are no MI on the right side of the diagonal line through the plot.

A sub data set of about one half hour was selected to be analysed in more detail. The corrections of the IGS in (x,y,z,t) were compared with the broadcast message to compute the IGS range correction, as is illustrated in Figure 5-2. Then the computation of the ENT-INT bias estimate was done by comparing, epoch by epoch, the corrections from IGS to ESTB, and estimating one bias for all satellites, as is illustrated in Figure 5-3. After all epochs have been processed the final result for the bias is shown in Figure 5-4.

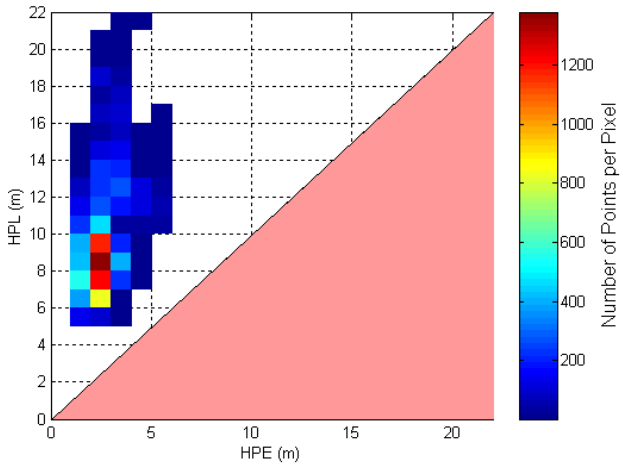

Figure 5-1 Protection level and position error in vertical direction for 10/25/01 at ESTEC/ESA

After the estimation of the ENT-INT bias, the WUL for each satellite at each epoch has to be found. An example of the SBAS range correction error as a function of location within the service area is shown in Figure 5-5. The WUL for 19:00:00 UT for PRN 11 was found to be at 25N,15W.

Finally the $5.33*\sigma_{flt}$ (Fast & Long Term Error bound found from UDRE and degradations) value is plotted against the SREW values for all satellites in view during the time interval. The result is shown in Figure 5-6. As with the XPL vs. XPE graphs, there are no cases of underbounding. As an example, the bounding for satellite PRN 7 are shown in Figure 5-7.

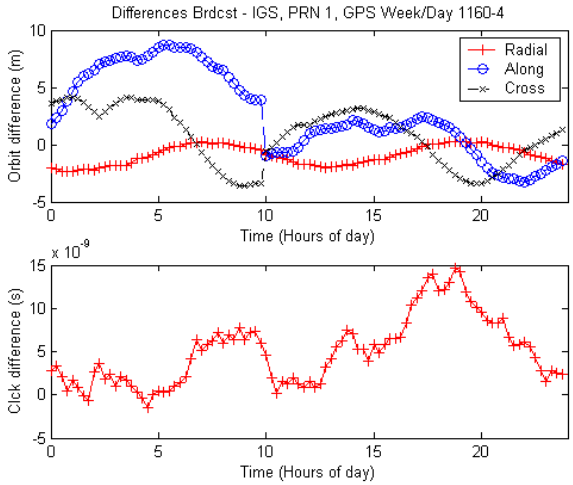

Figure 5-2 Comparison of navigation message to IGS orbit and clock data.

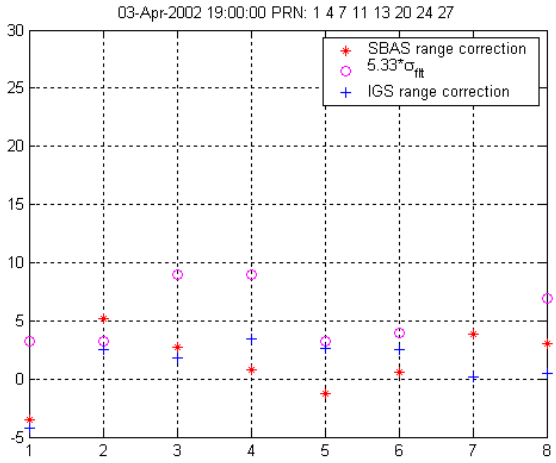

Figure 5-3 Corrections before ENT-INT bias adjustments

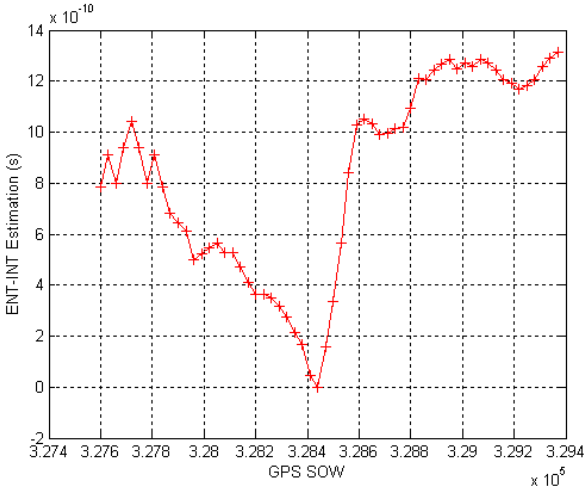

Figure 5-4 ENT-INT Bias estimation

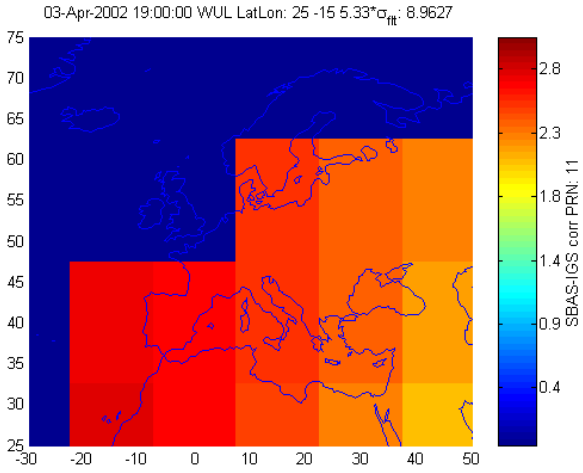

Figure 5-5 Finding the WUL at a certain epoch for PRN 11

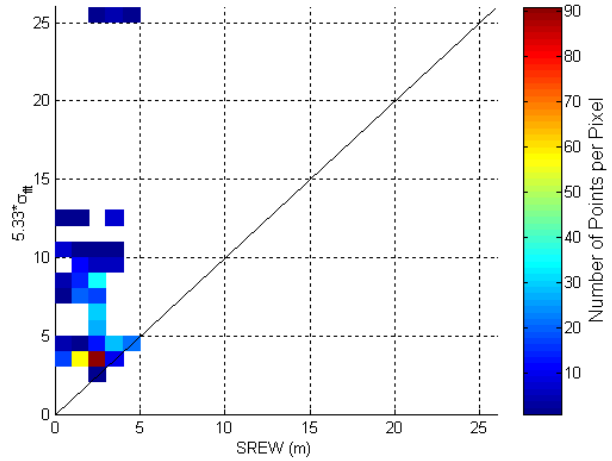

Figure 5-6 5.33*σ_{flt} against SREW for all satellites in view

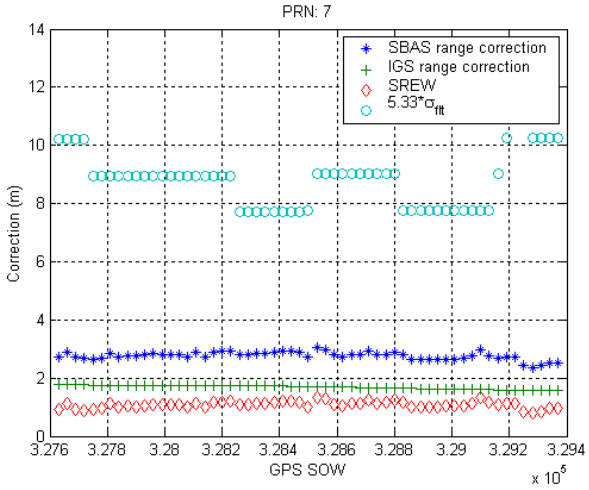

Figure 5-7 Corrections, SREW and 5.33*σ_{flt} vs. time for PRN 7

5.1 IONOSPHERIC INFORMATION

The same time interval as before can be analysed for the ionospheric delay and error indication bounding, using the method described in section 4. As can be seen in Figure 5-8, which is representative for the entire period, there is no integrity violation found from the ionosphere data, as all values are positive (overbounding).

5.2 MULTIPATH AND RECEIVER NOISE ANALYSIS

The multipath and receiver noise analysis for the MI epoch did not reveal any values above the expected from the [DO-229C] standard as is shown in Figure 5-9. The red line represents the MOPS [DO229-B] assumptions on combined multipath/receiver noise for class 3/4 equipment with $\sigma_{i,noise}$=0.5 and $\sigma_{i,mp45}$=0.25 m, according

to Eqn. 5-1. Note that i denotes a certain satellite and ele stands for the elevation.

$$\sigma^2_{i,air} = \sigma^2_{i,noise} + \frac{\sigma^2_{i,mp45}}{\tan^2(ele_i)} \qquad \text{Eqn. 5-1}$$

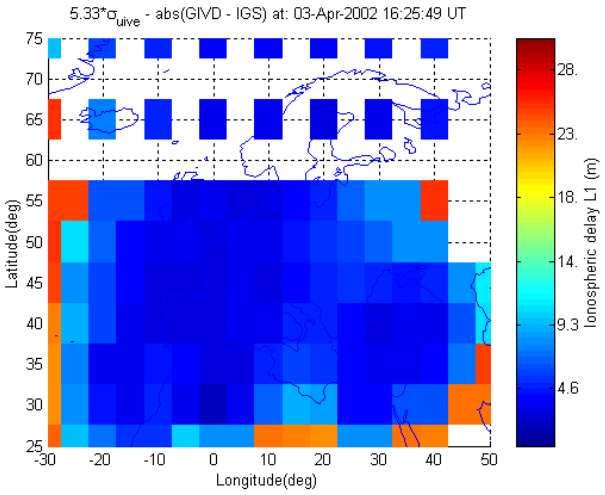

Figure 5-8 Ionospheric data comparison of ESTB to IGS for the MI epoch.

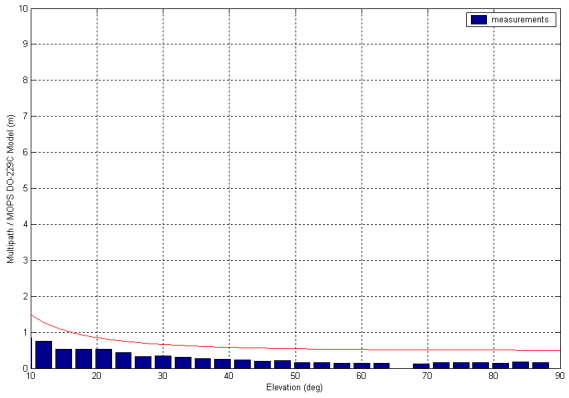

Figure 5-9 Multipath + receiver noise as function of the elevation for all satellites in view for the MI epochs

6 DEMONSTRATION OF METHODOLOGY ON ESTB / WAAS BOUNDING ANALYSIS

The WAAS system, currently broadcasting in testing mode and operational for non-safety of life applications, may also be considered to assess the validity of the proposed verification techniques (e.g. to highlight properties of the bounding characteristics of GIVE/UDRE.) The objective of this section is to show that the methodology described in Section 4 also works when applied to the WAAS broadcast signal. As a spin-off of this assessment, we also compare some signal format and performances of ESTB and WAAS systems.

Note: The assessment performed here corresponds to ESTB SIS as broadcast early April 2002. Under ESA Contract, a new ESTB software release is currently under development by GMV. This should be operational by next July 2002. The main evolutions offered to users are: the addition of corrections for the GEO Inmarsat AOR-E (PRN 120), the update of the messages broadcast in order to comply with the standard RTCA [DO-229B], the robustness of the system aiming at providing 95% of time the SIS and the addition of messages type 6 and 17 in the SIS [ESTB2].

6.1 MESSAGE CHARACTERISTICS

In this section we compare the WAAS and ESTB at message level only, without having to make position solutions. This comparison is divided into direct comparison of message content and absolute comparison of the message content of both systems against a third party reference. Messages are received from WAAS (AOR-W PRN 122) and ESTB (AOR-E PRN 120) at ESTEC with a DSNP Aquarius and a Novatel Millenium receiver.

	ESTB				WAAS			
MT	**%**	**MIN**	**MAX**	**MEAN**	**%**	**MIN**	**MAX**	**MEAN**
0	20.00	5.00	13.00	5.97	16.70	1.00	6.00	5.29
1	1.01	90.00	120.00	118.05	1.80	1.00	43.00	13.14
2	20.00	5.00	18.00	5.97		N/A		
3	20.00	5.00	18.00	5.97	16.70	1.00	6.00	4.86
4	20.00	5.00	18.00	5.98	N/A		N/A	
7	1.06	90.00	120.00	112.60	0.97	19.00	108.00	68.71
8		N/A			0.96	54.00	95.00	71.29
9	1.33	85.00	95.00	90.02	1.17	68.00	77.00	72.86
10	1.02	85.00	120.00	117.49	0.96	40.00	91.00	66.71
12	0.46	215.00	454.00	261.24		N/A		
17		N/A			0.37	145.00	275.00	235.14
18	1.38	5.00	220.00	86.26	3.48	1.00	6.00	1.71
24		N/A			16.70	1.00	6.00	5.29
25	7.80	5.00	54.00	15.31	9.00	1.00	41.00	11.04
26	6.00	1.00	90.00	19.79	4.52	1.00	5.00	1.57
28		N/A			8.66	1.00	4.00	1.86
62		N/A			2.38	40.00	42.00	41.71
63		N/A			15.58	1.00	100.00	6.42

Table 6-1 WAAS and ESTB Message broadcast intervals (sec)

The analysis of the broadcast intervals of the messages revealed the following differences, as can be concluded from Table 6-1:

- WAAS currently uses MT28 as defined in [DO-229C]. In addition, use and definition of MT8 is not described in [DO-229A or B]. Note that MT 62 + 63 are test and null messages.
- WAAS is optimising the bandwidth by using MT0 as MT2, MT3, and MT24 instead of MT 4 and part of

MT25. This is due to the fact that these three messages can broadcast UDRE/PRC information up to 13+13+6=32 satellites which corresponds to the number of satellites declared as monitored in MT1. EGNOS on the contrary uses MT2, MT3 and MT4 to monitor up to 13*3=39 satellites whereas the mask of monitored satellites in MT1 normally contains only 29 satellites

Regarding the fast and slow corrections the following differences are detected analysing the raw messages:

- For ESTB the UDREi for the GEO (PRN120) is set at 14 (Not monitored) even if seen by most of the stations, whereas for WAAS the UDREi for AOR-W (PRN122) is set at 12 (99.4%), 13(0.4%) and 14 (0.2%) and the UDREi for POR (PRN134) is set at 12 (20.4%), 13(79.3%) and 14 (0.3%)
- From the fast corrections it can be seen that PRN 12 and PRN19 are declared as monitored by WAAS (whereas their UDREis are set at 14 (Do Not Use)) and not monitored by ESTB.
- ESTB and WAAS broadcast a UDRE degradation factor of 5.8mm/s^2 for all satellites. However the latency broadcast for ESTB is 7s and against 1s for WAAS.

Regarding the ionospheric information, the interpolation differences between MOPS [DO-229A and B] are not used, because bands 8 and 9 are not used in both systems. The GIVEs for both systems are shown in Figure 6-1, where the dark blue colour at the edges of the coverage area means 'not supported' instead of 0.

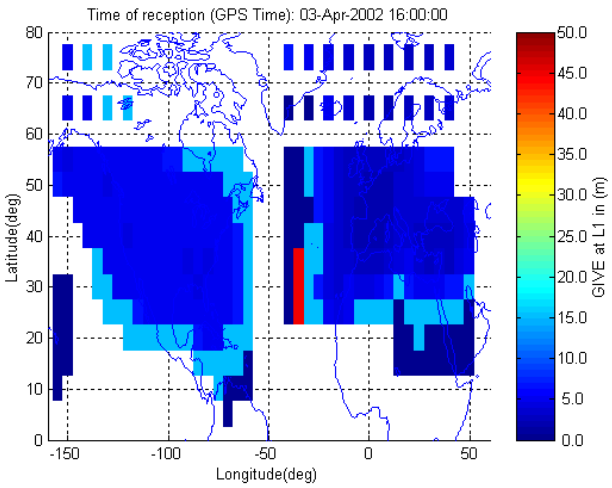

Figure 6-1 Example of ionospheric GIVEs transmitted for both ESTB and WAAS at the same time

6.2 PROTECTION LEVELS

Differences between WAAS and ESTB protection levels are expected a priori, but comparison might still give some useful insight.

In Figure 6-2 to Figure 6-5 below, the XPL values and integrity availabilities are plotted, computed by the ESA service volume tool ESPADA [ESPADA]. The data is collected at ESTEC from 03-Apr-2002 15:12:45 to 04-Apr-2002 03:13:06.

The XPL values are computed with the following assumptions on the [DO-229 B] Appendix J:

- The type of equipment used is Class 3/4, which means that the $\sigma_{i,air}$ is computed by Eqn. 5-1 with $\sigma_{i,noise}$=0.5 (GPS) and 1.0 (GEO), and $\sigma_{i,mp45}$=0.25 m.
- The assumed K values are taken for PA, Kh=6.00 and Kv=5.33.
- All visible and system-monitored satellites are used in the computation of the protection level with a mask angle of 5 degrees.

The conclusions that can be drawn from these figures is that for class 3/4 receivers:

- The vertical availability of integrity is the same for ESTB as for WAAS for a VAL of 50m (in civil aviation terminology corresponding to APV 1.5).
- The minimum VPL for WAAS is up to 6m higher than that for ESTB

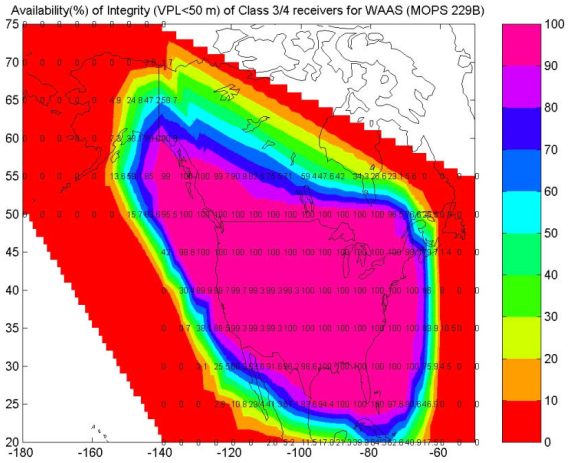

Figure 6-2 Availability of WAAS VPL below VAL=50m

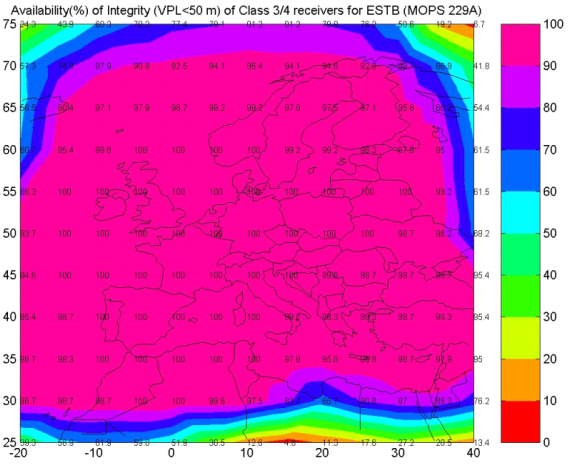

Figure 6-3 Availability of ESTB VPL below VAL=50m

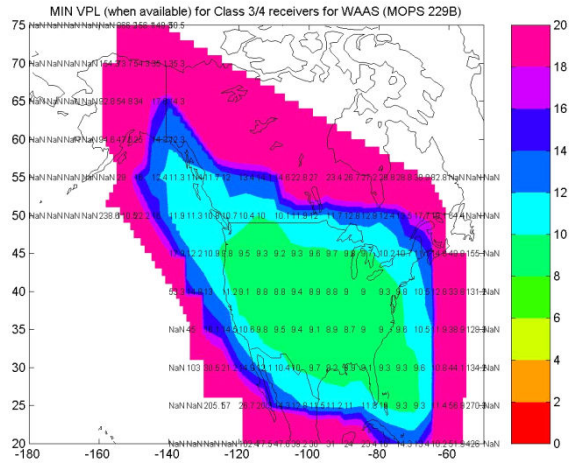

Figure 6-4 Minimum WAAS VPL for 12 hours

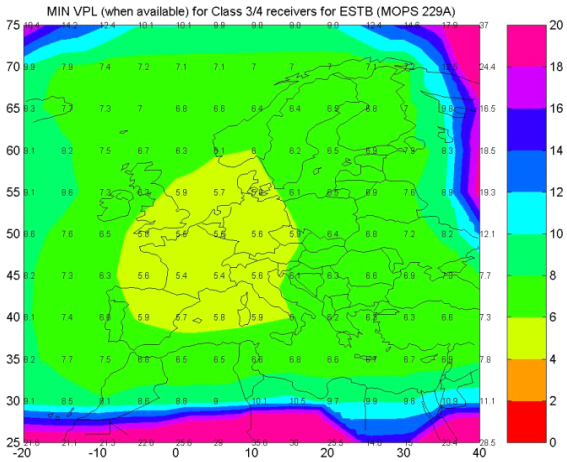

Figure 6-5 Minimum ESTB VPL for 12 hours

6.3 IONOSPHERIC BOUNDING

The same date was also analysed using the IGS IONEX files as a reference. The ESTB and WAAS measurements were collected at ESTEC from 03-Apr-2002 15:15:00 to 04-Apr-2002 15:15:00.

The results are illustrated in Figure 6-6 and Figure 6-7. As expected the WAAS system is currently more conservative on the bounding of the ionosphere than the ESTB. During EGNOS GIVE algorithm testing, performed at EGNOS Critical Design review, those large margins on the ionospheric bounding are also observed.

These figures indicate that the technique for GIVD/GIVE verification using IGS data indeed also work for WAAS. The application also shows that ESTB, despite having fewer ground reference stations than WAAS, still manages to successfully overbound the real GIVD with very high precision.

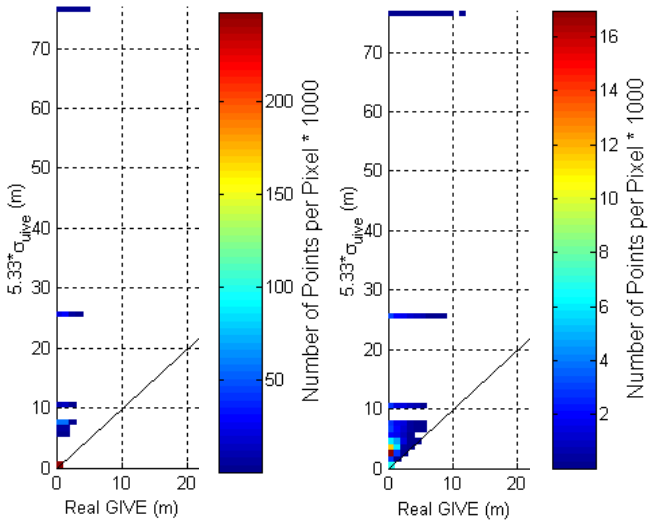

Figure 6-6 Real GIVE vs σ_{uive} values for all supported grid points for every broadcasted map of ionospheric information in WAAS on the left and ESTB on the right

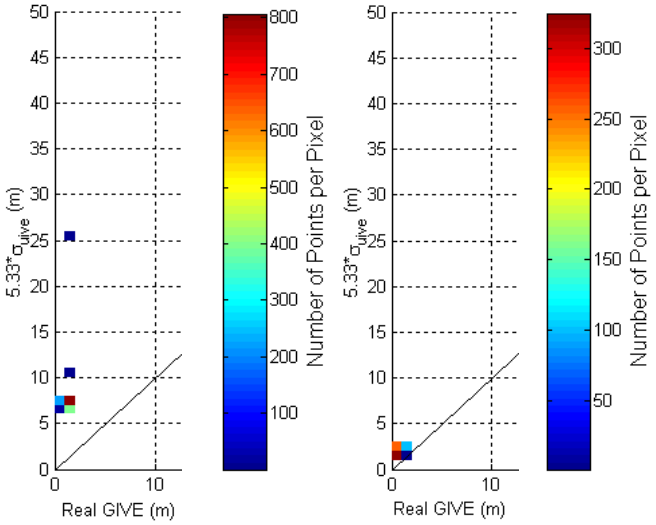

Figure 6-7 Real GIVE vs σ_{uive} values for (40N,110W) on the left (WAAS) and (40N,0E) on the right (ESTB)

7 CONCLUSIONS

In this article, system verification techniques that allow assessing SBAS integrity performances have been described and tested through the analysis of both the EGNOS test bed (ESTB) and WAAS broadcast signals. The use of the ESTB SIS has proven to be an excellent resource to asses and develop verification techniques, which will be, later on, applied to EGNOS.

A specific verification methodology to assess the individual bound capabilities of UDRE/GIVE/Local error bounds has been presented and its effectiveness demonstrated through the post processing of both ESTB and WAAS broadcast signals. As a spin-off of this assessment, it has been possible to compare the protection level bounding properties of both ESTB and WAAS, and to understand the source of the differences.

The excellent results obtained with the ESTB, a very reduced version of the final EGNOS system, are beyond initial expectations: accuracies close to 1m (2σ) [ESTB] and adequate protection level that bounds the real errors. The experience gained by ESA / Industry / CNES / NMA / EOIGs / EUROCONTROL on the ESTB development / performances, paves the way for a successful introduction of the EGNOS system at the beginning of 2004.

8 REFERENCES

[ESTB] ESTB Web site, www.esa.int/estb

[ESTB2] H. Secretan,. J. Ventura-Traveset, F. Toran, G. Solari and. S. Basker, EGNOS System Test Bed Evolution and Utilisation, ESA Workshop NAVITEC 2001, Dec. 2001.

[DO-229A] RTCA MOPS, (May 1998)

[DO-229B] RTCA MOPS, (October 1999)

[DO-229C] RTCA MOPS, (December 2001)

[IGS01] IGS Web Site, http://igscb.jpl.nasa.gov/

[IGS99] IGS Ann. Rep. 1999, http://igscb.jpl.nasa.gov/

[ION01] IONEX Format description and interpolation routines, http://www.aiub.unibe.ch/ionosphere.html

[ESPADA] F. Toran, J. Ventura-Traveset and J.C. de Mateo, "ESPADA 3.0: An innovative EGNOS Simulation Tool Based on Real Data," *ESA Journal preparing for the Future,* January 2002.

9 ACKNOWLEDGEMENTS

The authors wish to thank Francisco Amarillo Fernandez for his support on the assessment of satellite orbit and clock verification.